Journal of the Oceanographical Society of Japan
Vol. 35, pp. 9 to 25, 1979

Some Properties of Surf-beats*

Yukio FUJINAWA**

Abstract: Long ocean waves with periods of several minutes (surf-beats) were observed at a marine observation tower. We have analysed time series data of an envelope of incident swell, long period current velocity and surface elevation fluctuations. Current velocity was measued by an electromagnetic flow meter. Surf-beats amplitude $H^{(l)}$ is shown to be proportional to 3/2 power of incident swell amplitude $H^{(s)}$, and decreases with increase of depth h in proportional to $h^{-1/2}$ such that $H^{(l)} \sim H^{(s)}\ (H^{(s)}/h)^{1/2}$. Frequency energy density function $P_{LL}(f)$ of surface elevation had two dominant peaks whose frequencies were highly stable through the entire observational period. Cross-spectral analysis suggested that those peaks correspond to traveling edge waves caused by the excess momentum and mass flux in the surf zone. The forced long ocean waves predicted by LONGUET-HIGGINS and STEWART (1964) was ditected. Phase-shift and wave height of the wave with respect to those of incident swell envelope are shown to be in remarkable agreement with the predictions. However the forced long wave is only a minor component in the total energy of surf-beats. Current fields are shown to be largely composed of non-surface modes.

1. Introduction

Approaching the coastal region, the wind wave deforms and finally decays due to effects of the sea bottom. The dynamical processes in the surf zone induce various phenomena with periods much longer than that of the incident wind-generated wave. They are surf-beats, wave set-up, longshore current, rip-current and undertow. These phenomena are thought to be governed by the spatial and temporal horizontal distribution of radiation stress of the incident waves in the surf zone for given nearshore topography, and may depend on one another through nonlinear interaction. However, our knowledge about even an individual phenomenon is so limited that it is reasonable, now, to concentrate our effert on revealing some characteristics or origin of each phenomenon.

This paper treats the surf-beats. The surf-beats were noted first by a Japanese scientist Terahiko TERADA who is also known as a famous essayist. MUNK (1949), however, is the first who treated the surf-beats quantitatively. He measured long-period sea surface undulation and incident wind-generated waves, and showed that wave height of the surf-beats is nearly proportional to incident wave height with a coefficient of about 0.1. The surf-beats were attributed to the varying mass transport associated with the varying incident wind wave height. TUCKER (1950) measured the phase difference between the surf-beats and incident wave groups (an envelope of wind wave), and showed that a group with larger wave height of wind-generated waves corresponds to depression of the long waves. LONGUET-HIGGINS and STEWART (1964) predicted the existence of a long wave forced by varying radiation stress of wind waves, and suggested the surf-beat is a free long wave which is radiated from the surf zone when incident wave breaks there. They predicted phase relationship of long waves in relation to incident wave group which is in agreement with the observational result of TUCKER. In this paper, however, the long forced wave will be shown to be a minor part of the surf-beats.

GALLAGHER (1971) considered the surf-beat as an trapped edge wave induced by a nonlinear interaction of the incident wind-generated waves. Our analysis will support his claims partially.

Previous observations of the surf-beats were usualy confined to the measurement of the surface elevation due to long waves and wind-generated waves. In the present study, hori-

* Received June 28, 1978, revised Jan. 8 and accepted Feb. 21, 1979.

** Institute of Coastal Oceanology, National Research Center for Disaster Prevention, 9-2, Nijigahama, Hiratsuka, Kanagawa 254, Japan

zontal velocities were also measured as well as the surface elevation of long waves and wind-generated waves in the hope that the surf-beats will be more definitely studied. Moreover, spectral analysis is used to decompose the long-period motion.

2. Preliminary analysis

The coordinate system is taken as in Fig. 1. The x_2-axis is taken along a straight coastal line on the static horizontal plane, x_1-axis extends seawards perpendicular to x_2-axis on the same plane and x_3-axis taken vertically upwards. Bottom topography is represented by

$$x_3=-h(x_1, x_2) \qquad (1)$$

The wind-generated wave comes from $x_1=\infty$, is modified as they approach the coastal region and breaks at the breaking point x_{1b}. The region $x_1<x_{1b}$ is called the surf zone.

If there exists excess mass transport M_α, in the long wave approximation continuity equation is

$$\frac{\partial \zeta}{\partial t}+\frac{\partial Q_\alpha}{\partial x_\alpha}=-\frac{\partial M_\alpha}{\partial x_\alpha}\equiv G_1 \qquad (2)$$

where $Q_\alpha\,(\alpha=1, 2)$ is the horizontal mass transport, and ζ water surface elevation.

Momentum equation are

$$\frac{\partial Q_1}{\partial t}+gh\frac{\partial \zeta}{\partial x_1}=+\frac{1}{\rho}\frac{\partial}{\partial x_1}(S_{33}-S_{11}) -\frac{1}{\rho}\frac{\partial S_{12}}{x_2}+\frac{1}{\rho}\tau_s{}^{(1)}-\frac{1}{\rho}\tau_b{}^{(1)}\equiv G_2 \qquad (3)$$

$$\frac{\partial Q_2}{\partial t}+gh\frac{\partial \zeta}{\partial x_1}=+\frac{1}{\rho}\frac{\partial}{\partial x_2}(S_{33}-S_{22}) -\frac{1}{\rho}\frac{\partial S_{12}}{\partial x_1}+\frac{1}{\rho}\tau_s{}^{(2)}-\frac{1}{\rho}\tau_b{}^{(2)}\equiv G_3 \qquad (4)$$

where S_{ij} is the vertical integration of the Reynolds stress due to the fluctuating motion, τ_s surface stress and τ_b bottom stress.

In the surf zone the turbulence caused by the wave breaking must contribute to the term S_{ij}, which is almost entirely equal to the radiation stress in the open ocean.

As a matter of fact, the shallow water approximation used in the present treatment becomes invalid in the region far from the shore ($x_1\to\infty$). Uniformity of an approximation should be carefully examined in case of the consideration of nonlinear effect as treated by WITHAM (1976). However the problem is beyond the scope of the present study.

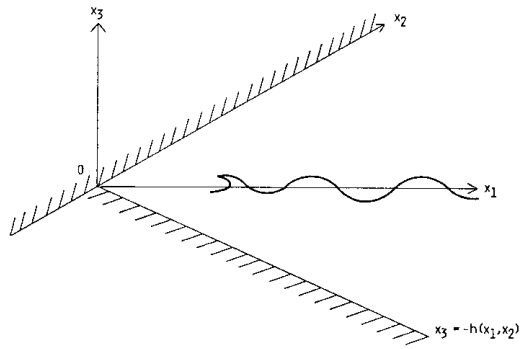

Fig. 1. Coordinates system taken in an analysis of dynamical processes near the surf zone.

Eqs. (2)-(4) constitute a system of partial differential equations to determine three unknown quantities ζ, Q_1, Q_2. Boundary conditions are that of zero mass transport at the shore $x_1=0$,

$$Q_1=0, \text{ at } x_1=0 \qquad (5)$$

and that of no motion at infinity,

$$Q_\alpha,\ \zeta\to 0, \text{ at } x_1 \qquad (6)$$

If we consider a phenomenon which is independent of the alongshore direction, equations for ζ and Q_1 are,

$$\frac{\partial \zeta}{\partial t}+\frac{\partial Q_1}{\partial x_1}=-\frac{\partial M_1}{\partial x_1} \qquad (7)$$

$$-\frac{\partial Q_1}{\partial t}+gh\frac{\partial \zeta}{\partial x_1}=-\frac{1}{\rho}\frac{\partial S_{11}}{\partial x_1}-\frac{1}{\rho}\tau_b{}^{(1)} \qquad (8)$$

In the absence of bottom stress, we obtain a solution

$$\rho\zeta=\frac{S_{11}}{gh-c^2{}_g} \qquad (9)$$

where c_g is the group velocity of the wind-generated wave (LONGUET-HIGGINS and STEWART, 1964). The long period surface undulation is caused by inhomogeneous distribution of radiation stress. They attributed the surf-beats to this quasi-static undulation due to incident waves. We will consider this type of

waves quantitatively by the use of the observational data in a later section.

Similar system of equations were treated by REID (1958). If the bottom profile is simplified as,

$$h(x_1, x_2)=sx_1,\ s\ll 1 \tag{10}$$

The eigenvalue problem was solved as

$$\begin{aligned}\zeta&=H(x_1;\ k,\omega)e^{i(kx+\omega t)}\\ Q_1&=U_1(x_1;\ k,\omega)e^{i(kx+\omega t)}\\ Q_2&=U_2(x_1;\ k,\omega)e^{i(kx+\omega t)}\\ H&=a_nq_n(\xi)\\ \xi&=2kx_1\end{aligned} \tag{11}$$

(REID, 1958), where a_n is the wave amplitude at the shore, and $q_n(\xi)$ is the Laguerre function of order n. The function is represented by the Laguerre polynomial $L_n(\xi)$ as

$$q_n(\xi)=\frac{e^{-\xi/2}}{n!}L_n(\xi) \tag{12}$$

Since the function $q_n(\xi)$ decreases rapidly seawards ($\xi\to\infty$), this solution represents a wave trapped along the shore, that is an edge wave.

We shall show that the surf-beats are mainly composed of the trapped edge wave as stated by GALLAGHER (1971). However his edge wave is driven by the nonlinear effect of the incident wind-generated wave, so that the period of the edge wave is nearly twice that of the incident wave as in the case considered by BOWEN (1969). It is common that periods of the surf-beats are an order larger than those of incident waves (MUNK, 1949; TAKAHASHI *et al.*, 1971; GODA, 1975). Then it is unreasonable to think that surf-beats are driven by a nonlinear effect of the incident wave. As is suggested from (2)-(4) the edge wave (surf-beats) is thought to be driven by the excess fluxes of momentum and mass caused by the inhomogeneous temporal and/or spatial wave field.

In the forced problem, an solution is expressed by use of eigenfunctions as,

$$\zeta=\sum_{n=0}^{\infty}\int_{-\infty}^{\infty}A_n(k,t)H_n(x_1, x_2, t;\ k)\,dk \tag{13a}$$

$$Q_1=\sum_{n=0}^{\infty}\int_{-\infty}^{\infty}A_n(k,t)U_n(x_1, x_2, t;\ k)\,dk \tag{13b}$$

$$Q_2=\sum_{n=0}^{\infty}\int_{-\infty}^{\infty}A_n(k,t)V_n(x_1, x_2, t;\ k)\,dk \tag{13c}$$

where,

$$A_n(k,t)=A_n(k)+\int_0^t M_n(k,t')dt' \tag{14}$$

$$M_n(k,t)=\int_{-\infty}^{\infty}dx_2\int_0^{\infty}\left[\frac{1}{gsx_1}\times\{U_n^*G_2+V_n^*G_3\}+H_n^*G_1\right]dx_1 \tag{15}$$

If we assume

$$G_i=g_i(x_1)e^{i(lx_2+\sigma t)} \tag{16}$$

M_n can be written as

$$\begin{aligned}M_n&=e^{i(\sigma-\omega_n)t}\,2\pi\,\delta(l-k)\Xi_n\\ \Xi_n&=\int_0^{\infty}\{(U_n^*g_2+V_ng_3)/gsx_1+H_n^*g_1\}\times dx_1\end{aligned} \tag{17}$$

where δ is the Dirac delta function. Contribution from radiation stress term g_2, g_3 seems weighted towards the shore. However, as is easily shown

$$V_n,\ U_n\sim H_n/x_1$$

so that there is no difference between radiation stress and mass flux term in the excitation of edge waves in the surf zone. Edge waves which satisfy the resonance condition

$$\omega_n=\sigma,\ k=l \tag{18}$$

will attain much larger amplitude than non-resonant ones.

3. Method and observation

Long-period surface elevation and horizontal-flow velocities were measured as well as water pressure variation due to short-period swell. Water pressure variation was measured by a Vibrotron-type pressure gauge, and two components of horizontal velocity were by an electromagnetic current meter with a sensor of disk type. The sensors of the wave gauge and the current meter were attached to marine observation tower about five meters beneath the mean water level. To pick up informations concerning the long period motions, we used an active electronic filter whose cut-off periods

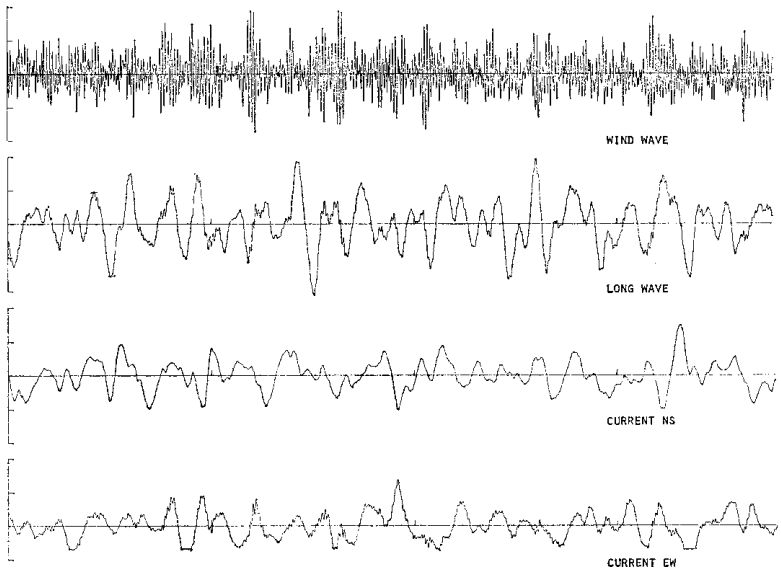

Fig. 2. An record of observation of surf-beats. Uppermost curve shows surface fluctuation due to incoming swell, second long period surface undulation due to the surf-beats, third offshore (NS) component of long period current fluctuation and forth alongshore (EW) component of current fluctuation.

are 100 and 1,000 seconds. Signals from the band-pass-filters were amplified, and then digitized by an A/D converter. Digital data were transmitted through a submarine cable to the laboratory on land and gathered by a computer NEAC-3200. Data were sampled at every 2 seconds. The tower and laboratory had air-conditioners. It was checked up that the variation of temperature in the rooms caused by the air-conditioners did not affect output signals from the present observational system.

Bottom contour line around the tower is nearly parallel to the shore line. Water depth around the tower is about 20 m, and the tower is some 1 km away from the shore. The geological feature of the sea bottom is fine sand.

Fig. 2 shows a sample of record obtained during the observation. The uppermost curve is the surface elevation due to the incident swell. The lower three curves are the surface elevation, north-south and east-west component of the flow field caused by the surf-beats. We will analyse these four time-series data to reveal characteristics of the surf-beats.

Observation was conducted nearly eighty hours from 20:45, Aug., 29, to 6:20, Sept., 2 in 1974. The observation covered a full evolution of the surf-beats from the initial stage of small amplitudes to the final stage of decaying with the most developed state in between. Significant wave height of the wind-generated wave reached about three meters, and the period was nearly fifteen seconds. The swell had very long crest length. Wind direction around the tower was opposite to that of incident swell with the maximum velocity of about twelve meters. A run contains 2,000 data, and analysis is conducted for each run.

4. Some statistics of the surf-beats

Swell attained its maximum height at about mid-night of the 31, August, and decayed as the typhoon moved westward. Trend of wave height of surf-beats $H^{(l)}{}_{max}$ shows good correspondence with that of incident swell $H^{(s)}{}_{max}$ as were the cases with MUNK (1949) and TUCKER (1950).

Before discussing quantitative relation between wave height of surf-beats and incident swell, we shall see relations between several kinds of statistics of surf-beat. The maximum wave height $H^{(l)}{}_{max}$ of the surf-beats is plotted versus the significant wave height $H^{(l)}{}_{1/3}$ in Fig. 3. The two quantities are seen to be related nearly

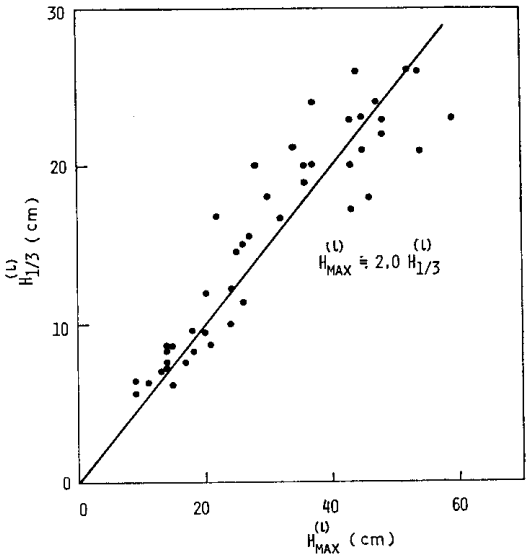

Fig. 3. Relation between the highest wave height $H_{max}{}^{(l)}$ and the significant wave height $H_{1/3}{}^{(l)}$ of the surf-beats.

Table 1. Proportional coefficients between various mean quantities concerning the surf-beats.

	Surf-beats			Current (offshore)		Current (alongshore)	
	$H_{1/10}$	$H_{1/3}$	$\overline{H}$	$H_{1/3}$	$\overline{H}$	$H_{1/3}$	$\overline{H}$
H_{max}	1.4	2.0	4.3	1.8	3.7	2.5	6.3
$H_{1/10}$		1.5	3.1	1.4	2.9	1.7	4.3
$H_{1/3}$			2.3		2.1		2.7

in a linear manner, though scatter of points is considerable. Ratios between various mean quantities (maximum $H^{(l)}{}_{max}$, significant $H^{(l)}{}_{1/3}$, (1/10) heighest mean $H^{(l)}{}_{1/10}$ and mean $\bar{H}^{(l)}$) of surface elevation due to the surf-beats are shown in Table 1. Scatter of data from a linear relation was very small in the cases of $H^{(l)}{}_{1/3}$ versus $H^{(l)}{}_{1/10}$ and $\bar{H}^{(l)}$ verses $H^{(l)}{}_{1/3}$. Table 1 also contains approximate ratios between satistical quantities concerning long period velocity fluctuations. It is remarkable that proportional coefficients concerning the surface elevation and those concerning current velocity are considerably different. If the long period water motin is entirely due to a kind of long waves the statistical characteristics of both surface elevation and current velocities will be nearly the same. We are led to a conclusion that large non-surface mode current fluctuation

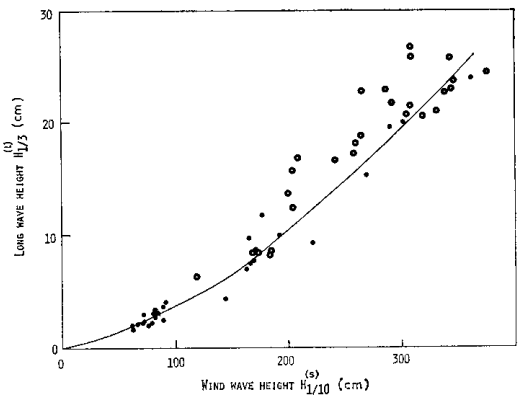

Fig. 4. Relation between one-tenth wave height $H_{1/10}{}^{(s)}$ of the incident swell and the significant wave height $H_{1/3}{}^{(l)}$ of the surf-beats. Symbol (○) corresponds to an developing stage, and (●) corresponds to an decaying stage.

(turbulence) is induced by the near-shore dynamical processes associated with the wind-generated wave decay.

Fig. 4 is a simultaneous plot of significant wave height of the surf-beats $H^{(l)}{}_{1/3}$ and the one-tenth wave height of the incident swell $H^{(s)}{}_{1/10}$. In the figure data are divided into those corresponding to a developing stage and those to a decaying one. Surf-beats height is rather smaller in the decaying stage, but the differrence is not so distinct. In this paper we assume quasi-static condition. Two quantities $H^{(l)}{}_{1/3}$, $H^{(s)}{}_{1/10}$ are choiced by a consideration that the surf-beats wave height would be relevant to the magnitude of wave group of the incident swell. However, scatter of points in the graph is little reduced compared with the case in terms of maximum wave heights. It is remarkable that relation between the long wave height and the incident wave height deviates noticiably from a linear one.

Figs. 5a, 5b is a log-log plot of wave height of the incident swell $H^{(s)}{}_{1/10}$ and the surf-beats height $H^{(l)}{}_{1/3}$. From now on suffix (1/3) and (1/10) for the surf-beats height and the incident swell height, respectively, are dropped out. Fig. 5 is composed of data by GODA (1975) at three different sites and those of MUNK (1949) as well as the present data. From the data the relation between the two quantities is described as

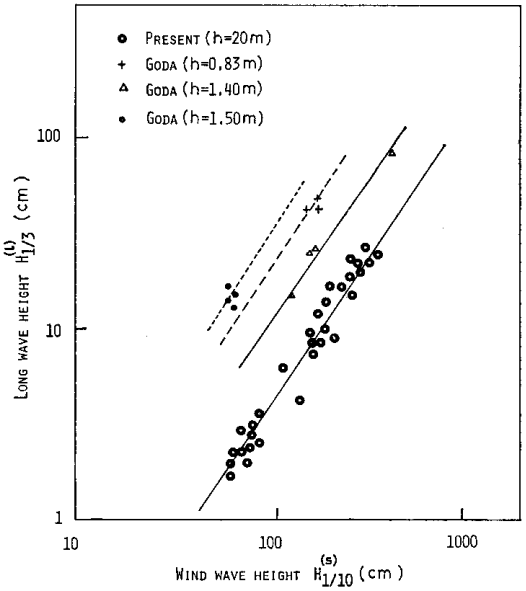

Fig. 5a. Log-log plots of surf-beats wave height $H^{(l)}$ *versus* the incident swell height $H^{(s)}$. Data are those of present observation as well as those of GODA (1975).

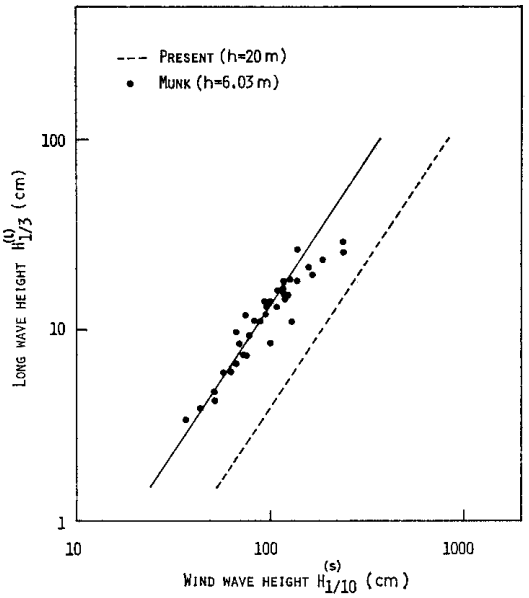

Fig. 5b. Same as Fig. 5a except data from MUNK (1949).

$$H^{(l)} \fallingdotseq \beta (H^{(s)})^{3/2} \qquad (19)$$

with a proportional coefficient β. The relation is markedly different from a linear relationship as noted by MUNK (1949) and TUCKER (1959).

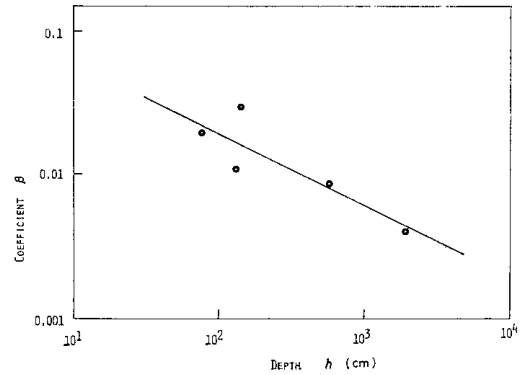

Fig. 6. Value of coefficient β in the relation $H^{(l)}=\beta (H^{(s)})^{3/2}$ *versus* observaional depth h. Data are tnose of GODA (1975), MUNK (1949) as well as that of present observation.

At a region of large wave height Munk's data deviate, however, from the relation (19) considerably. This may be explained by the presence of upper limit of the amplitude of the edge wave which is a main component of the surf-beats, as will be shown later. The range of Tucker's data is not so wide that his data are not inconsistent with the 3/2 power law (19).

Now take to consider the proportional coefficient β in the relation (19). Values of β are plotted versus the water depth h in Fig. 6. Almost all available data except those of TUCKER (1950) in which water depth h is not shown are used. From the figure we can guess,

$$\beta = 0.23/h^{1/2} \qquad (20)$$

Then, we can write down an empirical formula for the relation between the surf-beats height $H^{(l)}$ and the incident swell height $H^{(s)}$ as

$$H^{(l)}/H^{(s)} = 0.23\,(H^{(s)}/h)^{1/2} \qquad (21)$$

It is noted that the formula (21) is consistent with the assertions of MUNK (1962) that decay of the surf-beats amplitude with increase of water depth h is much stronger than the Green's 1/4 law and the water depth appears in the relation between the surf-beats height and the incident wave height in the form of $H^{(s)}/h$.

5. Spectral analysis of surface elevation and current velocity

It is suggested that the long period nearshore

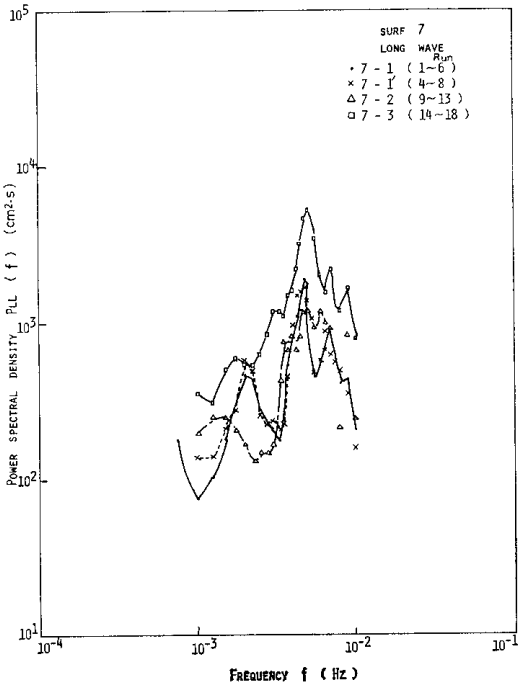

Fig. 7a. Energy spectral density function $P_{LL}(f)$ of the surface displacement due to the surf-beats for series 7-1 ~ 7-3. Existence of two sharp peaks and growth of them are noted.

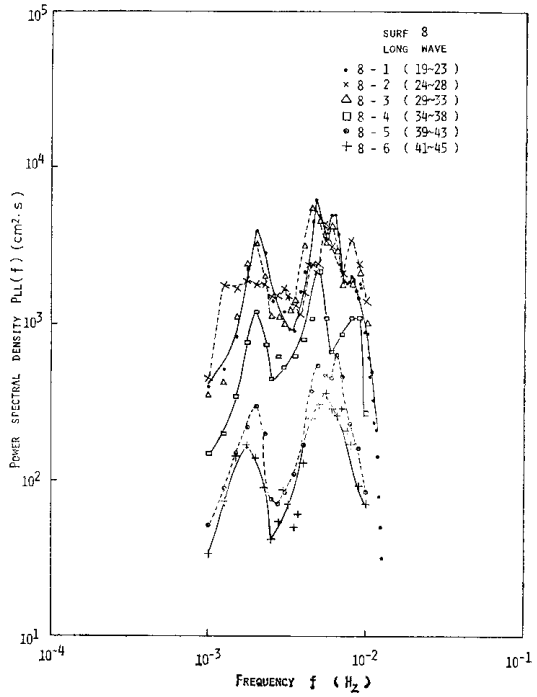

Fig. 7b. Same as Fig. 7a except series 8-1 ~ 8-6. High degree of similarity is evident.

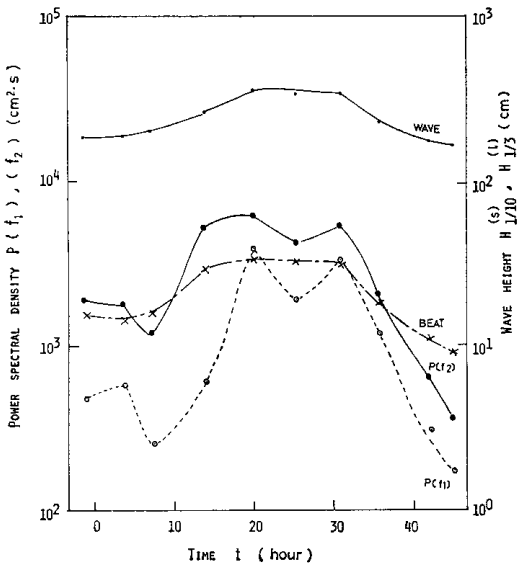

Fig. 8. Evolution of the incident wave height $H^{(s)}$ of swell, the surf-beats wave height $H^{(l)}$ and values of spectral densities $P_{LL}(f_1)$, $P_{LL}(f_2)$ of the two dominant peaks of spectral density function $P_{LL}(f)$ of the surf-beats. The component with frequency f_2 starts to develope earlier than that at the first peak. f_1 component attains an equilibrium value before the incident swell attains its maximum wave height.

water motion is composed of various modes. Figs. 7a, 7b show spectral density function $P_{LL}(f)$ of the surface elevation of the surf-beats for total series. Spectral analysis is done for each series with data length of four to six runs. Series 7-1, 7-1′ correspond to two adjacent initial stages, and series 8-1 to the most developed one. It is remarkable that there are two definite and dominant peaks in the spectrum. Frequencies f_1, f_2 of the peaks are nearly constant,

$$f_1 = 0.0020 \pm 0.00025 \text{ (Hz)}$$
$$f_2 = 0.0051 \pm 0.00038 \text{ (Hz)}$$

Variation of frequency of the peak at higher frequency is slightly larger, and its variation was systematic in time. Spectra of the surf-

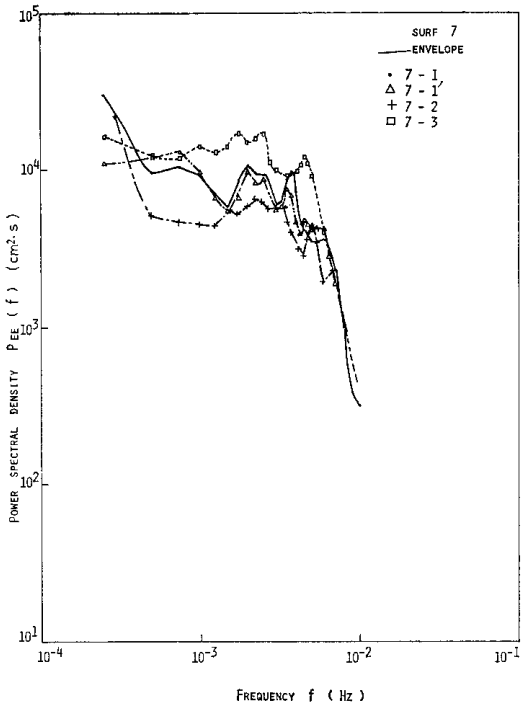

Fig. 9a. Energy spectral function $P_{EE}(f)$ of an envelope of surface displacement of the incident wave for series 7-1 ~ 7-3. It is remarkable that there is no stable dominant peak at the frequencies f_1, f_2 of the peaks which appear in the surf-beats spectrum.

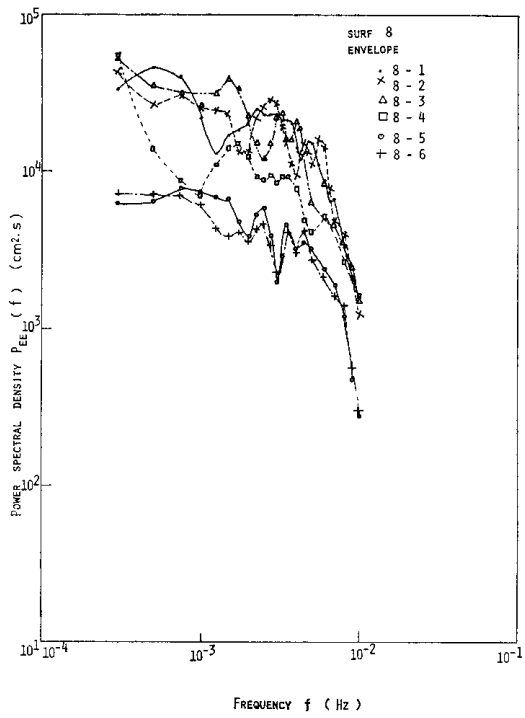

Fig. 9b. Same as Fig. 9a except series 8-1 ~ 8-6.

beats were also shown by MUNK (1962) and TAKAHASHI *et al.* (1971). Munk's spectrum is flat, but there are two definite peaks in the spectra of TAKAHASHI *et al.* at Tagonoura Port with very short period of 80~100 s and 38~47 s. Another remarkable feature in the spectra is the existence of a high similarity through the decay stage of the surf-beats.

Fig. 8 shows time evolution of power spectral densities $P_{LL}(f_1)$, $P_{LL}(f_2)$ at the two peaks, mean wave height $H^{(l)}$ of the surf-beats, mean wave height $H^{(s)}$ of the incident swell. It is evident that the higher frequency component

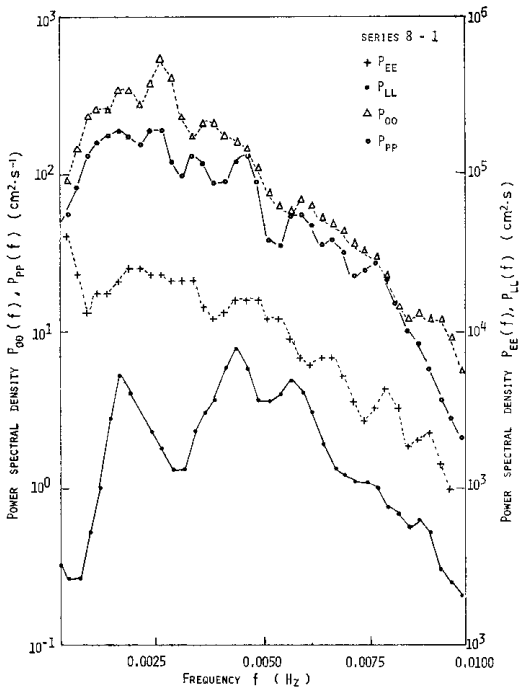

Fig. 10. Energy spectral density functions of→ long period surface and current fluctuation for series 8-1 which corresponds to the most developed case. P_{LL} shows surface displacement due to the surf-beats, P_{OO} offshore component of the velocity fluctuation, P_{PP} alongshore component and P_{EE} envelope of the incident swell.

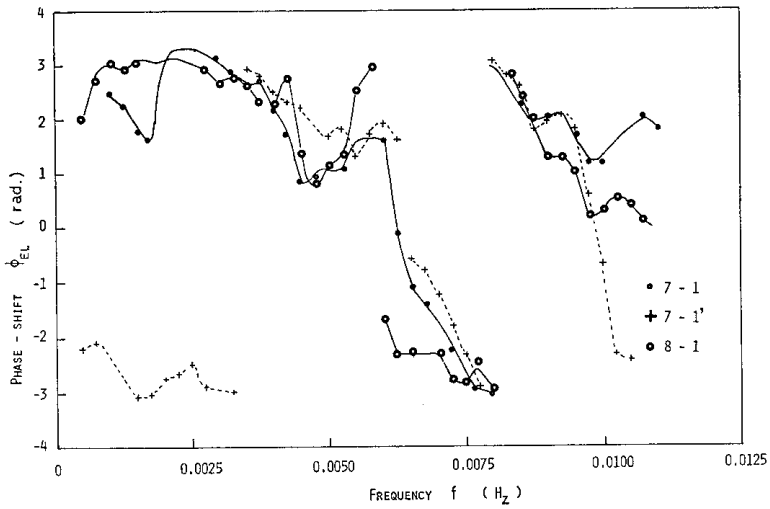

Fig. 11a. Coherence distribution $\gamma^2_{EL}(f)$ between an envelope of the incident swell and the surface displacement due to the surf-beats. Note existence of several peaks in the distribution. They are situated nearly in the frequency domain where the surf-beats energy $P_{LL}(f)$ is small. Note also the existence of large coherence in a higher frequency region (f= 0.008 Hz).

started to grow earlier than the lower frequency one, and attained an equilibrium magnitude definitely before the incident swell reached its maximum height. The lower frequency component (f_1) attained a maximum height simultaneously with the incident wave. Lapse times needed to attain maximum values are 10, 7, 10 hours for f_1 components, f_2 component and the incident waves, respectively. It is remarkable that there exists an upper limit of power spectral density $P_{LL}(f_2)$ for f_2 component. It might be due to an accelerated drainage of energy of the surf-beats to other mode by some nonlinear interaction.

Now we shall see whether the structure of the surf-beats spectrum can be explained simply from a similar structure of the incident swell spectrum. It is certain that the swell spectrum contained two peaks at the earliest time. But the higher frequency peak soon became negligibly small compared with the growing swell from the distant typhoon. We can say that the two peak structure of the surf-beats spectrum is not caused by the spectral form of the incident swell so long as we are confined within a quasi-stationary treatment.

If the forced long wave associated with the

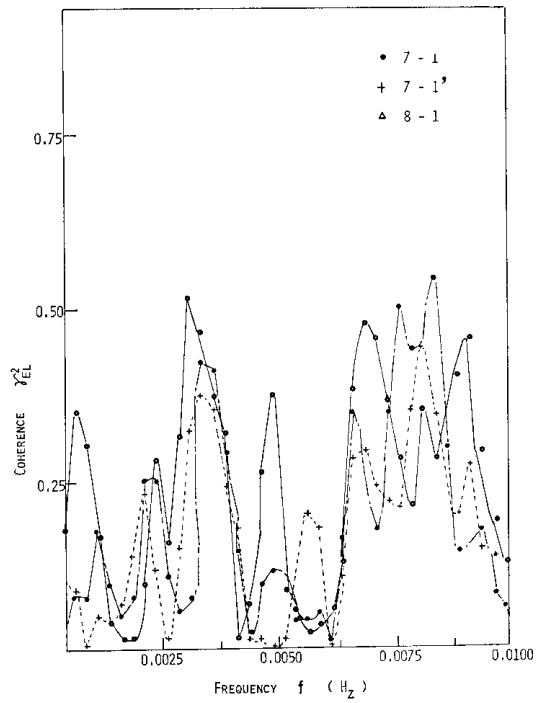

Fig. 11b. Phase-shift distribution $\phi_{EL}(f)$ between an envelope of the incident waves and the surface displacement due to the surf-beats. It is noted that $\phi_{EL}(f)$ is near π rad. in various frequency regions.

varying radiation stress of wind-generated wave field (LONGUET-HIGGINS and STEWART, 1964) is the dominant component of the surf-beats we can expect high degree of similarity between spectra of the surf-beats and wave-group spectrum. We take as a time series of wave group an envelope $e(t)$ of the surface elevation $\xi(t)$ of the incident swell

$$e(t)=\frac{1}{T_r}\int_t^{t+T_r}\xi(t)dt \qquad (22)$$

As a moving average time T_r, 80 s is adopted.

Figs. 9a, 9b are the power spectral density functions $P_{EE}(f)$ of envelope. The spectrum is very flat compared with that of surface elevation due to the surf-beats $P_{LL}(f)$, especially around the frequency region of the two peaks. We may say that the surf-beats are not predominantly consisted of the forced long wave caused by the varying radiation stresses of the incident wind wave field.

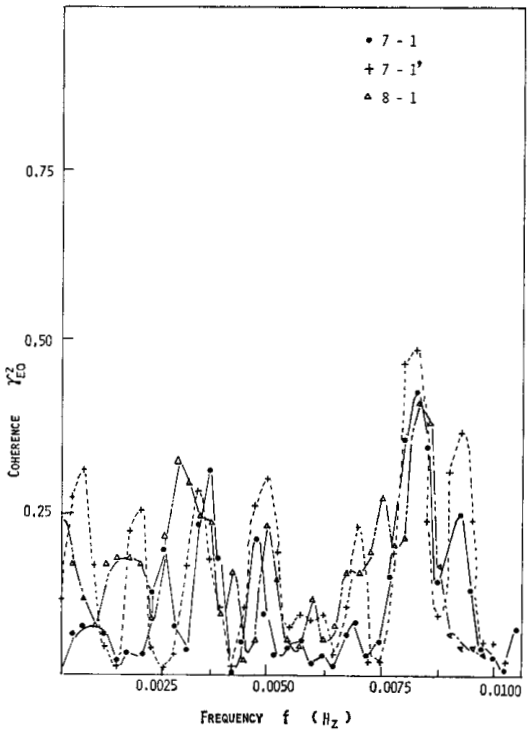

Fig. 12a. Coherence distribution $\gamma_{EO}(f)$ between an envelope of the incident wave and the offshore component of the velocity fluctuation. The coherence γ^2_{EO} is large in the high frequency region where $\gamma^2_{EL}(f)$ is large.

In Fig. 10 are shown power spectral density functions $P_{OO}(f)$, $P_{PP}(f)$ of the off-shore and alongshore components of long period current velocity. An eminent feature is that those spectra contain no sharp peaks unlike spectra of the surface elevation $P_{LL}(f)$. This distinct difference between spectra of current and surface elevation does show that horizontal current motion is largely composed of the non-surface mode. This current fluctuation may be due to internal waves or turbulence originated in the surf zone. Current field $\boldsymbol{u}$ is thus decomposed into,

$$\boldsymbol{u}=\tilde{\boldsymbol{u}}+\boldsymbol{u}',\ |\tilde{\boldsymbol{u}}|\ll|\boldsymbol{u}'|$$

where $\tilde{\boldsymbol{u}}$, $\boldsymbol{u}'$ are velocities associated with motion of surface mode and non-surface mode, respectively. It is also noted that there is poor similarity between successive spectra of current velocities $P_{OO}(f)$, $P_{PP}(f)$ unlike spectra of surface elevation $P_{LL}(f)$. Alongshore velocity spectrum $P_{PP}(f)$ contains somewhat clear peak

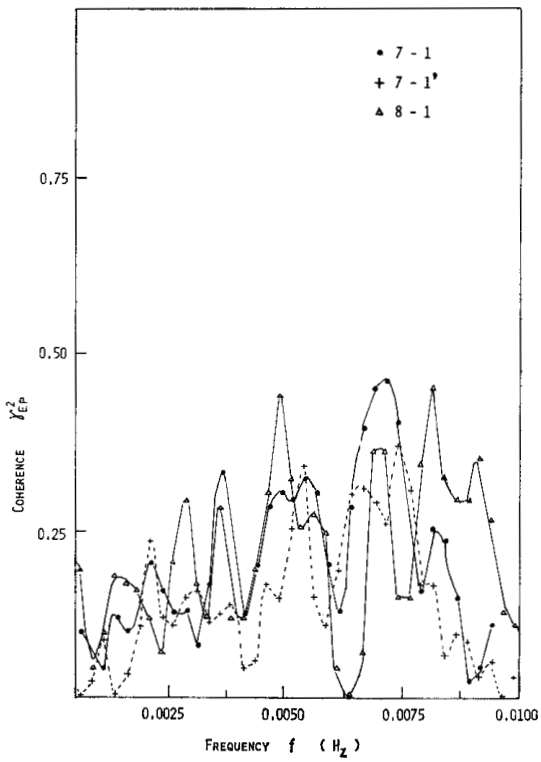

Fig. 12b. Coherence distribution $\gamma^2_{EP}(f)$ between an envelope of incident wave and the alongshore component of velocity fluctuation.

at around frequency f_2. However offshore velocity spectrum $P_{oo}(f)$ does not contain any peak there. It is suggested that a considerable part of the alongshore current at around the frequency f_2 are of surface mode. This will become clear when cross-spectral analysis of surface elevation and current velocity are made.

6. Cross-spectral analysis

Fig. 11a is the phase-shift between an envelope of incident swell $e(t)$ and long period ocean surface fluctuation $\zeta(t)$. Phase-shift $\phi_{EL}(f)$ is not a constant but varies in the frequency range concerned, and we are led to a conclusion that discussion of phase-shift between wave group and surf-beats elevation must be done on the basis of results of spectral analysis. Values of coherence γ^2_{EL} shown in Fig. 11b is nearly inversely proportional to the power spectral density $P_{LL}(f)$ of long wave. And, phase-shift $\phi_{EL}(f)$ is near π rad. at around the frequency region where coherence $\gamma^2_{EL}(f)$ is large, that is, crest of long wave corresponds to the smallest wave group. These situations will be exlained as follows. Spectrum of the forced long wave would be flat as the envelope spectrum $P_{EE}(f)$ as predicted by LONGUET-HIGGINS and STEWART (1964). Then, the forced long wave would be dominant at the frequency region of small surf-beats energy $P_{LL}(f)$ with the phase-shift of π rad. Small value in coherence $\gamma^2_{EL}(f)$ at the dominant peaks of the surf-beats suggests that the surf-beats is not mainly composed of the forced long wave induced by the variation of wave group. We must also note that there exists a frequency region of large coherence at a higher frequency range. Energy at the area is only a minor part of the total energy of the surf-beats. However, the forced mode is predominant at this higher frequency region. It is possible that energy in this region is shared by the reflected forced long wave. But the reflected forced long wave will have low correlation with the 'instantaneous' wave group since the wave group would be modified as each wave component does not undertake uniform modification as approaching to the surf zone.

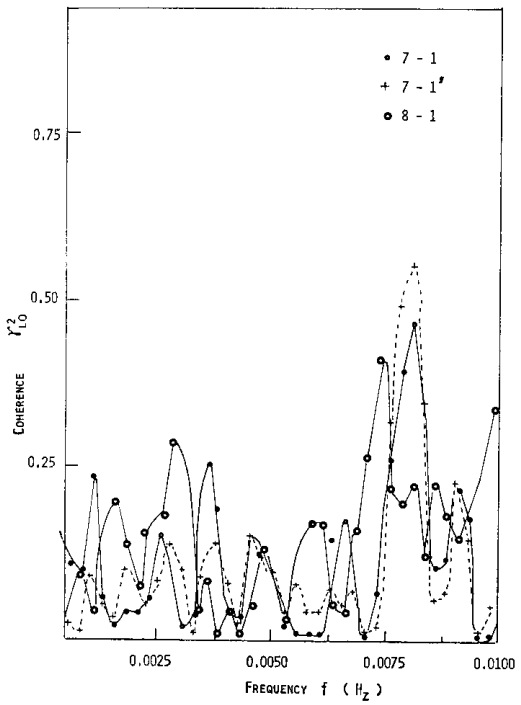

Fig. 13a. Coherence distribution $\gamma^2_{LO}(f)$ between surface displacement due to the surf-beats and the offshore component of velocity fluctuation. There exists a large value of $\gamma^2_{LO}(f)$ near 0.008 Hz.

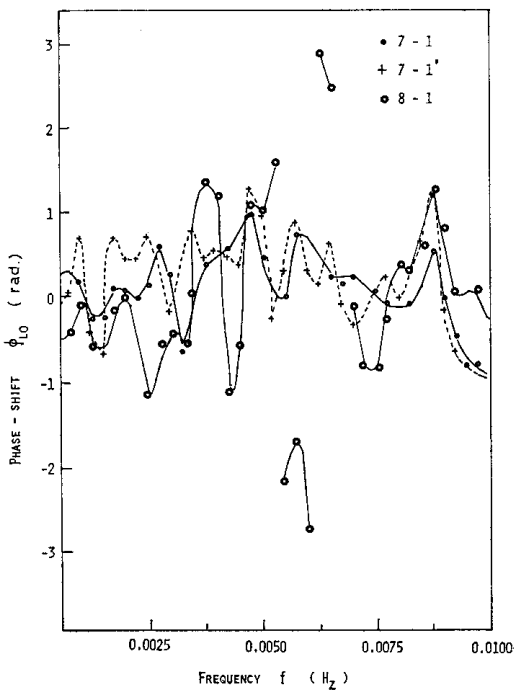

Fig. 13b. Phase-shift distribution $\phi_{LO}(f)$ between surface displacement and the alongshore component of velocity fluctuation.

Figs. 12a, 12b show coherence $\gamma^2_{EO}(f)$ between the envelope and offshore velocity component, $\gamma^2_{EP}(f)$ between the envelope and alongshore component, respectively. Smallness of $\gamma^2_{EO}(f)$ at the lower frequency range indicates that water motion in this frequency range is only slightly originated from the varying radiation stresses due to the incident swell. Presence of large value of $\gamma^2_{EO}(f)$ at a higher frequency region is an another evidence that water motion corresponding to these frequency is the surface mode which does not accompany any water surface elevation originated from the wind wave radiation stresses.

Largeness of the coherence $\gamma^2_{EP}(f)$ at a higher frequency indicates that there exist alongshore forced waves. However, smallness of $\gamma^2_{LP}(f)$ (though is not shown) at the frequency region casts doubts against the above reasoning.

Figs. 13a, 13b are the results of the cross-spectral analysis between surface elevation of the surf-beats $\zeta(t)$ and long period offshore velocity component $u(t)$. Coherence $\gamma^2_{LO}(f)$ and phase-shift $\phi_{LO}(f)$ are shown in Figs. 13a, 13b, respectively. Coherence $\gamma^2_{LO}(f)$ is small at around the dominant peaks of the surf-beats spectrum, which indicates that current in these range is largely due to the non-surface water motion. On the other hand, at a higher frequency range ($f \fallingdotseq 0.008$ Hz) $\gamma^2_{LO}(f)$ is very large showing once more that water motion in this frequency range is largely due to the surface mode. Phase-shift $\phi_{LO}(f)$ is nearly zero at the higher frequency though with considerable scatter of data points. The value $\phi_{LO}(f)$ reaches nearly zero around the region where coherence $\gamma^2_{LO}(f)$ is large.

Coherence $\gamma^2_{LP}(f)$ and phase-shift $\phi_{LO}(f)$ between long period surface elevation $\zeta(t)$ and alongshore velocity fluctuation $v(t)$ are shown in Figs. 14a, 14b, respectively. Most remarkable feature is that coherence $\gamma^2_{LP}(f)$ is very large at the frequency f_2 of the second dominant peaks of the surf-beats spectrum. It does show

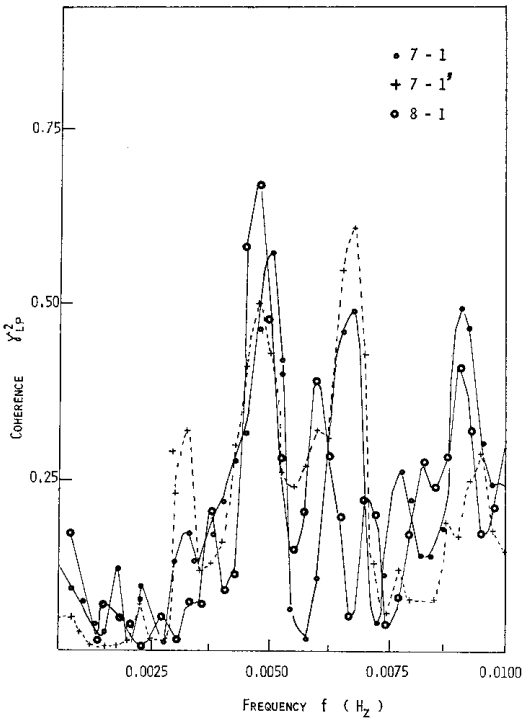

Fig. 14a. Coherence distribution $\gamma^2_{LP}(f)$ between surface displacement due to the surf-beats and the alongshore component of velocity fluctuation. $\gamma^2_{LP}(f)$ is very large at the frequency f_1 of the energy spectral peak of the surf-beats.

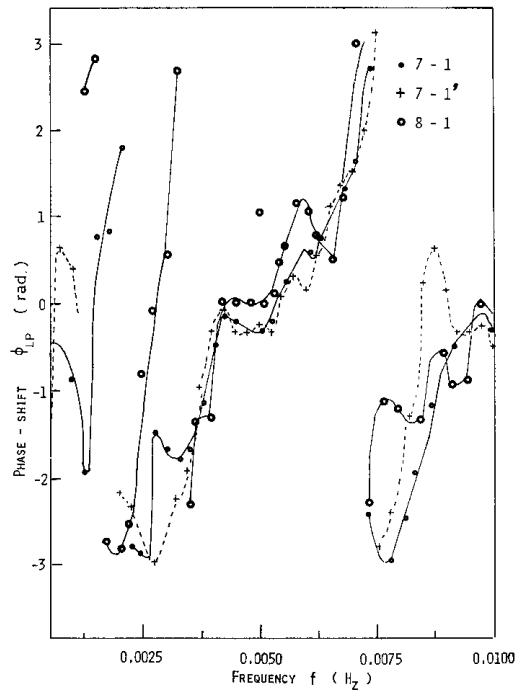

Fig. 14b. Phase-shift distribution $\phi_{LP}(f)$ between surface displacement due to the surf-beats and the alongshore component of the velocity.

that dominant component of the surf-beats is a wave whose motion is parallel to the coast. We may say that the wave is an edge wave trapped along the coast.

Smallness of $\gamma^2_{LP}(f)$ at higher frequency is another evidence that the motion in the frequency range is along x_1 axis coinciding with the direction of the incident swell.

In case of standing edge wave, phase-shift ϕ_{OP} of offshore velocity component u to the alongshore velocity component v, phaseshift ϕ_{LO} of surface elevation ζ to u are,

$$\phi_{OP}=0 \text{ (or } \pi),$$
$$\phi_{LO}=\pi/2 \text{ (or } 3\pi/2)$$

On the other hand, in case of travelling edge wave,

$$\phi_{OP}=\pi/2 \text{ (or } 3\pi/2),$$
$$\phi_{LO}=\pi/2 \text{ (or } 3\pi/2)$$

Our results show that dominant peak f_2 corresponds to an travelling edge wave. Mode of waves at the first peak f_1 could not be identified owing to the low coherence of $\gamma^2_{LO}(f_1)$, $\gamma^2_{LP}(f_1)$, $\gamma^2_{LE}(f_1)$. The low coherence is caused by the situation that power spectral densities of current $P_{OO}(f_1)$, $P_{PP}(f_1)$ at frequency f_1 is by far larger than that at f_2, and elevation spectrum $P_{LL}(f_1)$ is much smaller than $P_{LL}(f_2)$. However, we assume that f_1 component is also an edge wave mode.

By taking bottom slope s as

$$s=0.03$$

the alongshore wave length L_1 of the edge wave with frequency f_1 is,

$$L_1=1{,}900 \text{ m} \ldots . (n=0)$$
$$L_2=5{,}400 \text{ m} \ldots . (n=1)$$

observation by eye suggests the crest length just decaying is not larger than 2,000 m. For fixed frequency wavelength of the edge wave increases with mode number. And, wave number of the dominant edge wave would coincide with that of the dominant varying radiation stresses in the surf zone as a driving force. These situations lead to the conclusion that mode number n for f_1 is 0. Wavelengths of f_2 component are 280 m, 550 m, 1,100 m for mode number $n=0, 1, 2$, respectively. As is suggested from (15) amplitude A_n of the n-th mode wave could not be large when the magnitude of the driving force Ξ_n of (17) determined by the radiation stress distribution and eigenfunction is small. Offshore distribution $g_i(x_1)$ of radiation stress is thought to have a maximum at a point in the surf zone and reaches zero at $x_1=\infty$ and at $x_1=0$. Eigenfunction $q_n(\xi)$ has nodes when mode number n is larger than unity. So that A_0 would be the largest for the above inferred distribution of radiation stress in the near surf zone since the cancellation in integration do not occur.

NAGATA (1964) measured crest lengths of wind-generated waves. According to his results ratio of crest lengths to wavelength ranges from 0.2 to 0.6. Incident swell in our case had wavelength about 350 m. We get 1,700 m of crest length if the ratio is taken to be 0.2, which is in good agreement with lateral wavelength of 1,900 m for f_1 component.

Coherence $\gamma^2_{OP}(f)$ between offshore component and alongshore component of long period current is very small over the frequency range. It suggests that water motion is composed of alongshore and offshore component, and they are independent of each other.

We have shown that there does exist long forced wave generated by the varying radiation stresses of wind-generated wave as predicted by LONGUET-HIGGINS and STEWART (1964). Here we will study a quantitative relationship between the forced waves and the incident waves. In the frequency range

$$0.00775<f<0.00925 \text{ (Hz)}$$

the coherence $\gamma^2_{EL}(f)$ between incident wave group and the long ocean waves is extremely large as can be seen in Fig. 11b. We pick up the frequency f_R at which $\gamma^2_{EL}(f)$ is maximum. Then, power spectral density $P_{LL}{}^{(R)}(f_R)$ of the forced wave with frequency f_R directly relevant to the varying radiation stress at the observational point is

$$P_{LL}{}^{(R)}(f_R)=\gamma^2_{EL}(f_R)P_{LL}(f_R) \qquad (23)$$

Fig. 15 shows the plot of power densities of wave group $P_{EE}(f_R)$ and the forced wave $P_{LL}{}^{(R)}$. Data shows

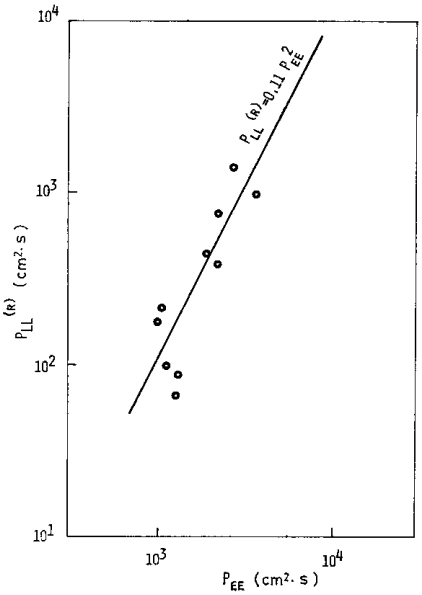

Fig. 15. Relation between energy spectral density $P_{EE}(f_R)$ of envelope of the incident swell and that $P_{LL}{}^{(R)}(f_R)$ of long period surface undulation induced by the varying radiation stress.

$$P_{LL}{}^{(R)} \fallingdotseq 0.11\, P^2{}_{EE} \qquad (24)$$

though with considerable scatter of points. Then amplitude of the long forced wave a_R is represented as

$$a_R = -0.33\, a^2 \qquad (25)$$

where a_R is the amplitude of incident swell. Negative sign is adopted from the observational result of phase-shift between envelope of incident waves and the long ocean wave in the frequency range. Moreover, for the present parameter of incident wave period ($T^{(s)}=15$s) and ocean depth ($h=20$ m) proportional coefficient in (25) calculated from the formula of LONGUET-HIGGINS and STEWART (1964) falls to be -0.32, which is in quite good agreement with the present value -0.33.

7. Discussion

Surf-beats amplitudes have been shown to be proportional to the incident wave amplitude. We must take into account of some dissipation mechanism to suppress surf-beats amplitude. A stationary state of a dominant edge wave with frequency σ and alongshore wave number l of amplitude $A_n(\sigma, l)$ which is resonating with the radiation stress field in the surf zone can be described as,

$$\frac{d}{dt}A_n(\sigma, l)=0 \qquad (26)$$

We can equate driving force term and dissipation term. We assume the bottom stress $\tau_s{}^{(\alpha)}$ is represented as

$$\tau_s{}^{(\alpha)} \sim (Q_i{}^{(\alpha)})^n \qquad (27)$$

Referring to the expressions for amplitude A_n (σ, l) in (14), (17), we get

$$(H^{(s)})^2 \sim (Q_i{}^{(\alpha)})^n \sim (H^{(l)})^n$$

By the use of the obtained result $H^{(l)} \sim (H^{(s)})^{3/2}$ as expressed in (21) we get

$$\tau_b \sim Q_i{}^{(\alpha)} |Q_i{}^{(\alpha)}|^{1/3} \qquad (28)$$

On the other hand, if use is made of the linear relationship as proposed by MUNK (1949) and TUCKER (1950), we get the familiar Chezy form,

$$\tau_b \sim Q_i{}^{(\alpha)} |Q_i{}^{(\alpha)}| \qquad (29)$$

We might infer that bottom stress formula for surf-beats is that of Chezy form (29) in the case of small amplitude, whereas in the case of large amplitude the stress formula is that of 4/3 power law effectively.

However as was also shown observationally, the second dominant peak of the surf-beats attained an equilibrium amplitude before the incident wave height took maximum value. This fact can not be explained by the simple dissipation mechanism $\tau_b \sim Q_i{}^n$. We must take into account of some nonlinear interaction mechanism. GUZA and BOWEN (1976) proposed a mechanism which gives a limit to the edge wave amplitude by transferring its energy to a long wave radiating offshore. We have shown that the forced long wave is arisen by the varying incident wave group. If the long wave are reflected at the shore as the incident swell decays there, the mechanism of Guza and Bowen may work.

We have seen above that the surf-beats is mainly composed of the edge wave of fundamental mode. On the other hand decay of the surf-beats with increasing depth is shown

to be well described by a $h^{-1/2}$ law. We should see if any contradiction exists between these two statements. For the edge wave of fundamental mode with wave number k, its amplitude $H^{(l)}$ changes with depth h as

$$H^{(l)} \sim e^{-kh/s}$$

Fig. 16 shows the ratio $H^{(l)}/(H^{(s)})^{3/2}$ versus $e^{-kh/s}$. Data are from GODA (1976), MUNK (1949) and the present observations. GODA (1976) observed at the three different observational sites, but only the case of swell type is used here. From the figure we can say that the $h^{-1/2}$ law is not inconsistent with the model of the surf-beats as edge wave of fundamental mode, and that the law is useful from the point of view of bulk treatment. However, it must be noted that data of GODA obtained in the condition of strong wind deviate largely from the line in Fig. 16.

SUHAYDA (1972) suggested a model of the surf-beats as the standing long waves of leaky mode. His siuation is that of finite length of bottom with constant slope, beyond which extends flat bottom to infinity. For homogeneous incident long wave spectrum, spectral density at a position within a sloping beach contains minimums whose frequency are independent of incident wave condition in agreement with the remarkable feature of the surf-beats spectrum in the present observation. SUHAYDA (1972) attributed the incident long wave to a wave generated from the nonlinear wave-wave interaction (HASSELMANN, 1962). However, period of the surf-beats is about an order larger than that of incident swell, so that such a large amplitude long wave would not be generated by the mechanism of HASSELMAN (1962).

Now take to see if the long forced wave generated by the mechanism of LONGUET-HIGGINS and STEWART (1964) constitutes the long standing waves as considered by SUHAYDA (1972). Fig. 17 shows the simultaneous plot of the power spectral density $P_{LL}(f_2)$ of the surf-beats at the secondary peaks and that $P_{LL}{}^{(R)}(f_2)$ of forced long wave at the same frequency. We can see that the observed energy of the surf-beats is several times larger than that of the incident forced long wave, which is against the idea of SUHYDA. High coherence between the surf-beats elevation and the alongshore current velocity as well as the sharpness of the spectral density of the surf-beats are not consistent with the model of SUHAYDA. It remains to be studied by which mechanism the radiation stress distribution contains such a fixed dominant wave number in spite of wide change of incident

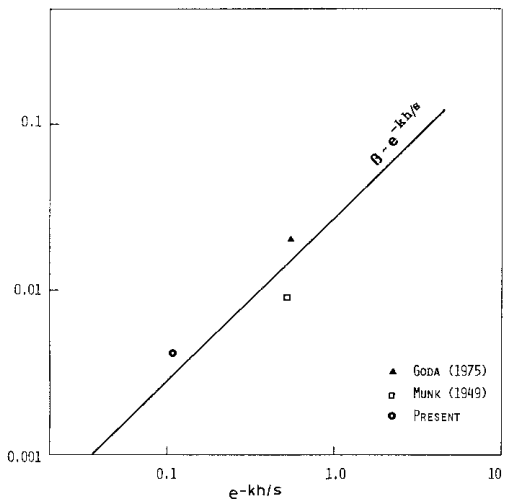

Fig. 16. Relation between β and $\exp^{(-kh/s)}$, where β is the proportional coefficient in the relation $H^{(l)}=\beta\,(H^{(s)})^{3/2}$.

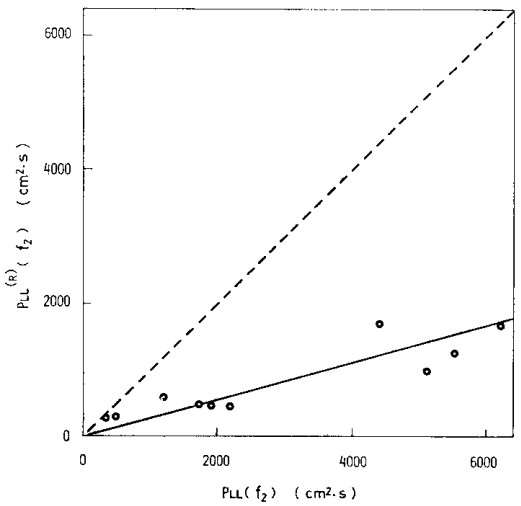

Fig. 17. Relation between energy spectral density $P_{LL}(f_2)$ at the second dominant peak of energy spectral density function $P_{LL}(f)$ of the surf-beats and the energy spectral density $P_{LL}{}^{(R)}(f_2)$ which is thought to be corresponding to the forced long wave.

wave condition. Bottom topography around an observation site may play an important role.

8. Conclusion

Following points are concluded by analysing the surface elevation and current velocities of long period (100s~1,000s) fluctuation in the surf zone.

1) Relations between the maximum 'wave' height H_{max}, the significant wave height $H_{1/3}$ of the surface elevation, and current of the surf-beats are nearly linear. The proportional coefficients are 2.0, 1.8 and 2.5 for elevation, offshore velocity component and alongshore component, respectively.

2) Waveheight of the surf-beats (significant) $H^{(l)}$ is related to the waveheight of the incident swell (mean of highest one-tenth) $H^{(s)}$ as

$$H^{(l)}/H^{(s)}=0.23\,(H^{(s)}/h)^{1/2}$$

where h is the water depth.

3) Spectral density of the surf-beats had two dominant peaks whose frequency remains nearly constant through the entire observational period more than eighty hours from the initial small wave condition to the last nearly quiescent condition through the largest incident wave height of some 3 m.

4) Through the decay stage, energy spectral density function of the surf-beats showed high similarity.

5) Higher frequency peak of the surf-beats attained an equilibrium energy considerably before the incident swell reached its maximum wave height. Some nonlinear mechanism may work.

6) The forced long wave caused by the varying radiation stress as predicted by LONGUET-HIGGINS and STEWART (1564) was observed. The phase and the wave height of the wave to those of the incident wave group were shown to be in good agreement with predicted values. However, the forced long wave is only a minor constituent in the total energy of the surf-beats.

7) Dominant peaks of the surf-beats were shown to be an edge wave of the fundamental mode travelling along the coast.

8) Current fields are overwhelmingly non-surface mode.

Acknowledgement

Thanks are given to Mr. Kenji OKADA who conducted large part of the experiment and to Mr. Isao WATABE who assisted greatly in the course of data analysis.

References

BOWEN, A. J. (1969): Rip Currents, 1. J. Geophys. Res., **74**, 5467-5478.

GALLAGHER, B. (1971): Generation of surf beat by non-linear wave interaction. J. Fluid Mech., **49**, 1-20.

GODA, Y. (1975): Rep. of Port and Harbour Res. Inst. **14**, 59.

GUZA, R. T. and A. J. BOWEN (1976): Finite amplitude edge waves. J. Mar. Res., **34**, 269-293.

HASSELMANN, K. (1962): On the non-linear energy transfer in a gravity wave spectrum Part 1. J. Fluid Mech., **12**, 481-500.

HASSELMANN, K. (1971): On the mass and momentum transfer between short gravity waves and longer-scale motions. J. Fluid Mech., **50**, 189-205.

LONGUET-HIGGINS, M. S. and R. W. STEWART (1964): Radiation stresses in water waves; a physical discussion, with application. Deep-Sea Res., **11**, 529-562.

MUNK, W. H. (1949): Surf beats. Trans. Amer. Geophys. Uni., **30**, 849-854.

MUNK, W. H. (1962): Long ocean waves. *In*, The Sea, Interscience, New York, pp. 647-663.

NAGATA, Y. (1964): Observation of the directional wave properties. Coastal Engine. in Japan, **7**, 11-29.

REID, R. O. (1958): Effect of coliolis force on edge waves (I). Investigation of the normal modes. J. Mar. Res., **16**, 109-144.

SUHAYDA, J. N. (1972): Experimental study of the shoaling transformation of waves on a sloping beach. Ph. D. dissertation, Univ. California.

TAKAHASHI, T., SUZUKI, Y., SASAKI, H. and NAKAI, T. (1971): Data of Port and Harbour Res. Inst. No. 130.

TUCKER, M. J. (1950): Surf beats; sea waves of 1 to 5 min. Period. Proc. Roy. Soc. A, **202**, 565-573.

WITHAM, G. B. (1976): Nonlinear effects in edge waves. J. Fluid Mech., **74**, 353-368.

サーフビートの特性について

藤　縄　幸　雄*

要旨: 平塚沖の観測塔で観測した周期数分程度の海洋波動（サーフビート）の特性を調べた．入射波浪の包絡線，長周期水位変動，水平2成分流速変動の四つの時系列のスペクトル解析を行った結果，次の諸点が明らかになった．

1) サーフビートの波高 $H^{(l)}$ は，水深 h の平方根に反比例し，$H^{(l)} \propto H^{(s)}(H^{(s)}/h)^{1/2}$ となる．ここに，$H^{(s)}$ は入射波浪の波高である．

2) 水位変動のエネルギースペクトルには，安定して二つの卓越したピークが存在する．

3) これ等のピークは，砕波帯内の radiation stress, mass transport によって駆動される進行性のエツジ波に対応する．

4) 波群の高低に伴う強制モードの波動が検出され，その大きさ，位相は，LONGUET-HIGGINS and STEWART (1964) の予想と大変よく合っている．

5) 流速の長周期変動は，大部分は非 surface モードから成っている．

* 国立防災科学技術センター平塚支所
〒254 神奈川県平塚市虹ケ浜 9-2